

# A numerical approach for a displacement-based ground support capacity consumption forecast

**S Dehkhoda** *Beck Engineering, Australia*

**F Reusch** *Beck Engineering, Germany*

**G Putzar** *Beck Engineering, Germany*

## Abstract

*The evolution and timing of discontinuous rock mass deformation is critical in evaluation of capacity consumption in individual support elements and overall performance of the support system. Ground support and reinforcement are installed in a strain free, or at a specified load condition (i.e. prestressed), into a deformed, discontinuous rock mass. The subsequent additional loads that develop in the support system are caused by additional displacements within the rock mass and the resultant forces generated by (i) blocks and wedges that would otherwise be kinematically free to fall or slide, and (ii) deformation of the continuum rock material between the discontinuities. Hence, the interaction between the support elements and the rock mass is complex and non-linear beyond the point of yield.*

*This paper reports on a numerical modelling technique that forecasts and assesses performance of ground support systems over the life of underground mining excavations. Simulating a support system in a discontinuous rock mass subjected to mining-induced stress and strain path, the authors have developed a methodology that tracks the consumed and the remaining capacity of the individual support elements within the system as loading demand increases. By providing a quantitative tool to assess performance of the support system over the life of mine, the outcome assists the mines to set guides to when and where preventative measures will be required. The results combined with closure forecast data also allow identifying high-risk areas and deformation trigger levels beyond which entry into an excavation with a particular support design would need to be reviewed. The modelling technique, set up and results are discussed in full within the paper.*

**Keywords:** *numerical modelling, ground support performance, capacity consumption*

## 1 Introduction

Emphases on displacement-based ground support design are increasing as more accurate and reliable ground deformation monitoring systems become available in mining operations (Lowther et al. 2022; Kaiser & Moss 2022). The key principle behind displacement-based design is to allow controlled deformation or displacement of the surrounding rock, ensuring that it remains within acceptable limits to prevent failure or collapse. This approach acknowledges that rock masses naturally deform and displace under stress and seeks to accommodate this movement while maintaining stability.

Displacement-based ground support design focuses on the behaviour of rock mass and aims to control or manage the displacement or deformation of the surrounding rock in response to mining activities. Hence the interaction between the ground support and the rock mass is a critical component in this design approach. The interaction between the support systems and the rock mass is, however, complex and becomes further complicated if the response beyond the point of yield of any of the components were of concern. This is mainly because the material behaviour is strongly non-linear post-yield and the failure of one part of the system could influence and/or lead to failure of another part. Numerical modelling techniques, such as combined finite–discrete element analysis (Munjiza 2004), are therefore useful tools to simulate the complex behaviour of the rock mass and assess the performance of different support systems.

The ground support simulation demands the highest level of realism. Apart from the quality of model input data (including material properties and boundary conditions), there are several modelling frameworks that can limit the ability of a simulation to reach realistic displacement values. The main categories of these characteristics to capture realistic ground support response are dimensionality, geometry, constitutive behaviour, and scale:

- **Dimensionality:** generally, displacement realistic models must be able to capture three-dimensional (3D) behaviour. When estimating the demand that a system will be subjected to, the complete 3D stress path, including its intermediate stages, is critical to the outcome.
- **Geometry:** capturing the geometry of a problem is essential to simulate the stress path. This means not only representing the excavation shape and structure, but also simulating the excavation timing. The process of forming the final geometry via several interim geometries will shape the extent and magnitude of damage and the deformation field. If the interim excavation stages are too far apart, i.e. the modelled excavation steps are too large, the simulation outcome cannot usually match the experience.
- **Constitutive model:** the effective constitutive response of a model is a function of the governing physics that a model can capture and account for. This is controlled by the constitutive material model, the numerical scheme, the solution mesh (including element type and density) or any other inherent characteristic that limits or constrains the behaviour of the simulated material.
- **Scale:** representative simulation of ground support response requires sub-models of mine scale models with excavations and discontinuities represented at a resolution and complexity suiting the smallest length scale of interest in the problem. The defined precision for deformation and distortion is critical to accurately generate the behaviour of discontinuous rock mass in tunnel scale. The resolution of the results reported in this paper are in the order of  $\sim 3$  or millimetres.

Assuming that a sufficient type and density of elements is used, and that the numerical framework can capture the required physical behaviour, the practical challenge for ground support modelling is to simulate the continuous and discontinuous parts of the deformation field around an excavation. This implies that the model will capture the stress–strain behaviour through simulating not only the extent and magnitude of damage around the excavation (for example with a strain softening, dilatant, large strain model), but also by incorporating sufficiently small-scale structures so that the discontinuous deformation and kinematics of the problem are reliably captured. The mentioned framework is tested with the simulation of a ground support system in a grizzly chamber and its surrounding excavations on a block cave extraction level as described later in the paper.

## 2 Methodology

The area of interest is a grizzly excavation and upper part of the orepass in a block cave mine. The geometry also includes important immediate excavations and extends further to minimise boundary effects on the results. The study simulates the effect of increased cave load on stress and damage around the excavations as the cave matures and, as a result, evaluates the performance of the built-in ground support system over the life of the excavations. The study uses submodelling technique with explicit finite element method to estimate stresses, strains and displacements including surface deformation effects. Starting with a large mine scale model, submodelling allows focusing on a particular part of the model to obtain results with greater accuracy. Displacement boundary conditions for the submodel are extracted from the results of the mine scale model, enabling a realistic stress path to be implemented. The submodel has the same number of modelling steps as the donor model to allow the simulation to correctly initialise and gradually evolve as boundary conditions are changed. This approach also eliminates sudden changes to boundary conditions which may appear if submodel was run at reduced number of steps.

The model geometry used in the study is shown in Figure 1a. The simulation is 3D with higher-order tetrahedral elements used for all volume elements.

## 2.1 Discrete structures

Discrete structures, large-scale faults and the local discrete fracture network (DFN) are represented by combining contact-cohesive elements to permit dislocations and separations on discontinuities while providing the correct kinematics of contact between the adjacent fracture surfaces. The main benefit of this is that the mechanics and kinematics of the contacts between the solid's continuous parts bound by cohesive elements is very well resolved and robustly solved, meaning the numerical solution is very stable and the representation of the stress–strain behaviour within rock parts need not be compromised to incorporate discontinuum behaviour.

An overview of the structures built into the model is shown in Figure 1b. These were implemented as two sets of DFNs that represented the local discontinuities and natural veining of the rock mass fabric. Considering the length scale of the problem (the target representative elementary volume [REV]) and to reduce meshing issues arising from small elements created by intersection of the discrete fracture surfaces, a lower bound threshold was applied to the DFN sets, neglecting any fractures smaller than 2 m persistence. In total, near 12,500 discrete fracture surfaces were explicitly built into the model. Smaller defects were represented by the homogenised continuum. The effect of this is that the REV of the model is <1 m, which is extremely small for a mining project.

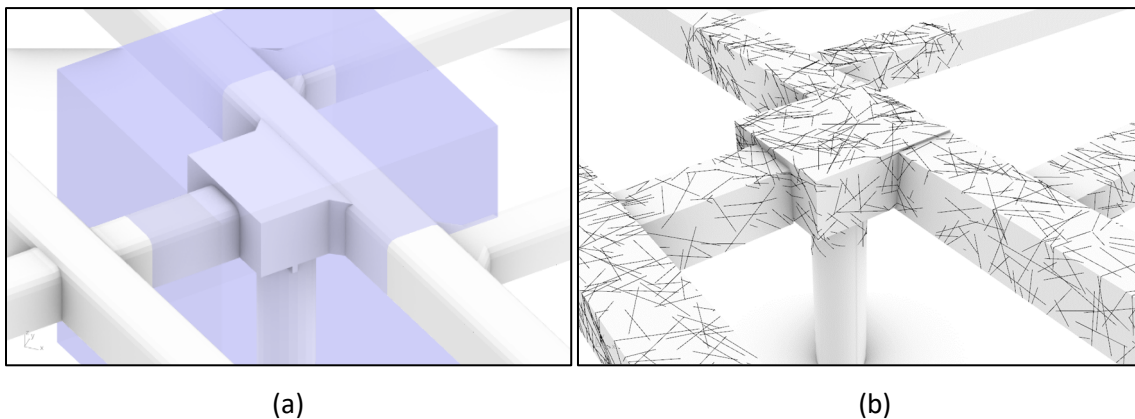


**Figure 1** (a) Submodel geometry. Box indicates the area of interest; (b) Overview of the traces of discrete structures built into the model

## 2.2 Ground support elements

Ground support elements studied in this paper are rockbolts (resin bars), cable bolts, mesh and fibrecrete (Figure 2). The ground support system at the excavations comprised of primary and secondary support elements as summarised in Table 1.

**Table 1** List of ground support elements

Excavations	Primary support	Secondary support
Chamber	3 m long rockbolts 1 × 1 m – 0.3 m from floor 75 mm in-cycle fibrecrete plus 8 mm mesh all over	6 m cables 1 × 1 m – 0.8 m from floor 50 mm fibrecrete to the ribs up to the height of 2 m plus 8 mm mesh in the bullnoses and camelbacks
Tunnels	2.25 m long rockbolts 1 × 1 m – 0.3 m from floor 75 mm in-cycle fibrecrete plus mesh all over	5 m cables 1 × 1 m – 0.8 m from floor 50 mm fibrecrete to the ribs up to the height of 2 m

Resin bars (fully grouted with solid steel bars) and cable bolts (fully grouted with steel strands) were explicitly built into the submodel as ‘beam elements’ with elastoplastic (von Mises-plasticity) properties. The lengths

of beam elements are in the order of 20–50 cm with circular cross-section, bending stiffness, and strain softening behaviour that is essential for modelling failure of the bolts.

All nodes are embedded in bulk rock which means technically no ‘slip’ is allowed between the beam and the volume (rock) elements. The slip and failure of the grouting (or snapping of the bolt) is modelled through appropriate setting of the beam properties (tensile strength versus elongation) which were selected based on the measured pull-out force versus pull-out distance. As those elements are integral part of the model, the simulation considers force feedback from bolt elements to the rock and vice versa, meaning rock and bolts affect each other.

Mesh and fibrecrete are modelled as shell elements and as one compound with homogenised elastoplastic properties. The thickness of the shell is selected based on the fibrecrete thickness and the shell properties were selected based on the combined mesh–fibrecrete system response. Displacement at the shell nodes is governed by the rock response. The model considers no force feedback to the rock from the surface support system since fibrecrete and mesh system can exert no major force on the rock (there is only negligible reaction force from fibrecrete and mesh to the rock).

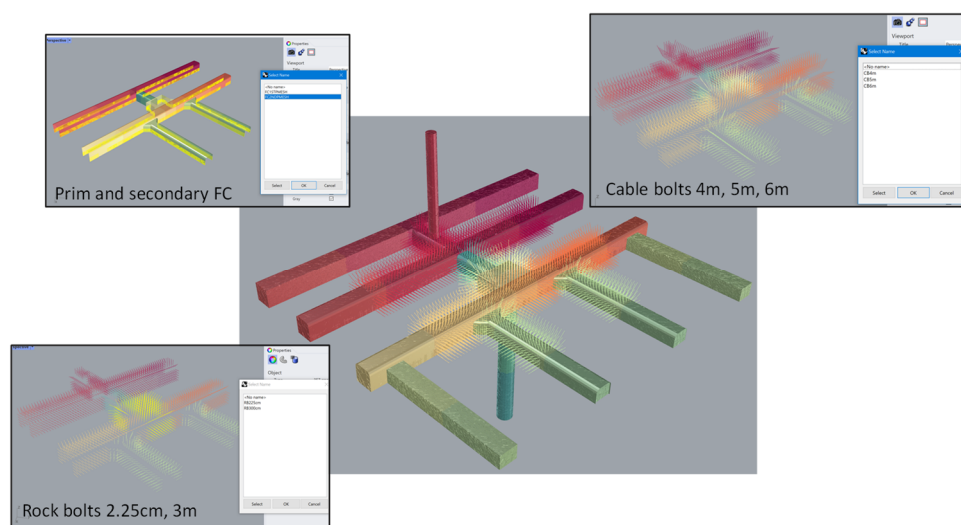


**Figure 2** Ground support elements incorporated in the model

### 2.3 Constitutive models and incorporated properties

The simulation components requiring constitutive model can be divided into four categories:

1. The continuum parts representing the intact rock or rock matrix between the discrete structure.
2. Discrete structures representing the discontinuities and rock fabric.
3. Rock and cable bolts.
4. Fibrecrete and mesh.

The rock matrix and continuum parts are modelled as strain softening dilatant materials using an extension of the Hoek & Brown failure criterion (Hoek & Brown 2019) that consider strain softening as described by Levkovitch (Levkovitch et al. 2010). Incorporation of the strain softening allows the material to soften, weaken and dilate as strain increases. Each geotechnical domain is defined by its own set of material properties, and all parameters for each rock type can vary at different rates with respect to strain changes, including the dilatancy parameter. This allows approximation of very complex stress–strain behaviour. In this study, single material type is considered.

Discrete structures have been implemented as cohesive elements. The Hoek–Brown failure criterion was used to determine 3D yield surfaces for discrete structures. The mechanical properties of the rock matrix and the discrete structures built into the submodel are listed in Table 2.

**Table 2** Representative elementary volume scale material properties for rock matrix and discrete fractures

Elements	$\rho$ (kg/m <sup>3</sup> )	UCS (MPa)	$\varphi$ (°)	C (MPa)	GSI	Level	$\varepsilon_{plast}$ (%)	E (GPa)	$\nu$	s	mb	a	e	Dilation	$\sigma_{crm}$
Rock matrix	2,700	160	–	–	84	PEAK	0	45	0.25	6.95E-02	5.39	0.5	0.6	0.4	42.13
						TRANS	1.75	35	0.25	4.50E-03	2.51	0.5	0.6	0.14	10.7
						RES	6.96	35	0.25	1.00E-03	1.48	0.5	0.6	0	5.05
LS Faults	2,750	0.16	25	0.5	–	PEAK	0	5	0.25	1	24	0.5	0.6	0.25	–
LS Faults	2,700	5	40	11.25	–	PEAK	0	37	0.25	2.08E-03	0.34	0.49	0.6	0.25	–
DFN-fabric	2,700	48	25	1.5	–	PEAK	0	37	0.25	2.08E-03	0.34	0.49	0.6	0.25	–

Rockbolts and cable bolts were defined as elastic perfectly plastic material based on the von Mises yield criterion. Its properties were adopted from in situ pull-out tests conducted on site. Table 3 shows the incorporated properties for rock and cable bolts within the submodel.

**Table 3** Implemented yield criterion for rock and cable bolts

Type	Diameter (mm)	Yield strength (MPa)	Displacements at yield (mm)	Stiffness (GPa)	Poisson's ratio
Cable bolts	15.2	1,860	25	40	0.3
Rockbolts	22.1	690	15	67	0.3

Fibrecrete and mesh were built as a combined compound in the submodel. The yield properties for the surface support system are shown in Table 4. No softening was considered for this system due to lack of confinement.

**Table 4** Combined fibrecrete and mesh surface support properties

Yield strength (MPa)	Stiffness (GPa)	Poisson's ratio	Thickness (mm)
5	20	0.2	75 and 50

### 3 Results and analyses

#### 3.1 Evolution of stress and damage

Stress distribution and damage during the service life of the excavations are shown in Figures 3 and 4, respectively. The frame numbers on the figures show different snapshots during the simulation process. The grizzly chamber experiences significantly higher stresses with major principal stress exceeding 120 MPa as the cave front approaches the drifts (see F040 in Figures 3 and 4). These high stresses can induce spalling and seismicity.

Moderate damage first evolves in the rib at the corners of the grizzly chamber (F040 in Figures 3 and 4) and as caving progresses, this extends to the backs (F050 in Figures 3 and 4). As damage grows, the stress relaxation zone around the excavation expands as well. Most of this damage is structurally controlled, meaning the governing mechanisms are shear/dilation on sub-excavation DFN surfaces. The slip along the large-scale fault also causes significant damage to the intersection of drift and panel drive.

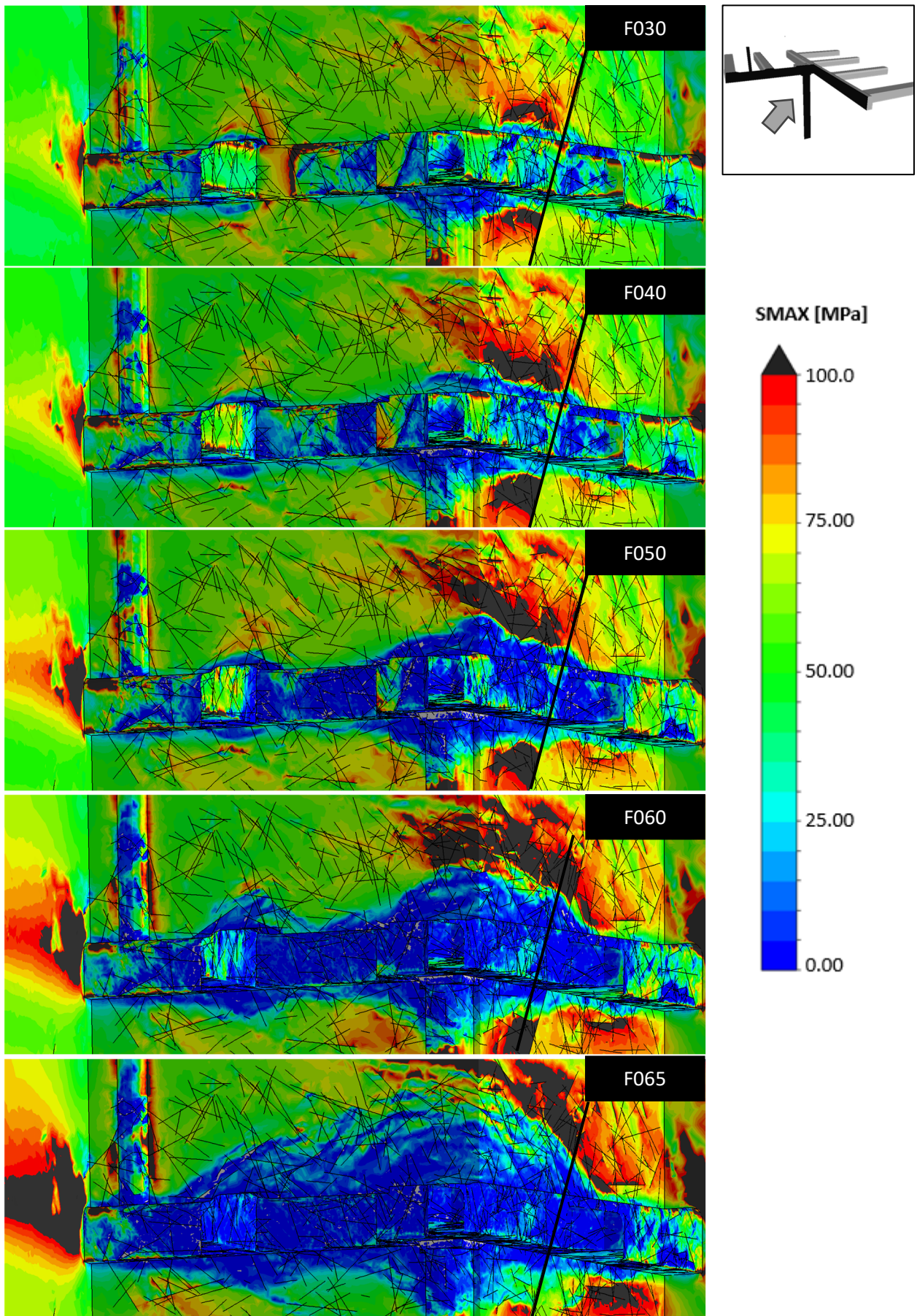


**Figure 3** Evolution of mining-induced stress around the excavations

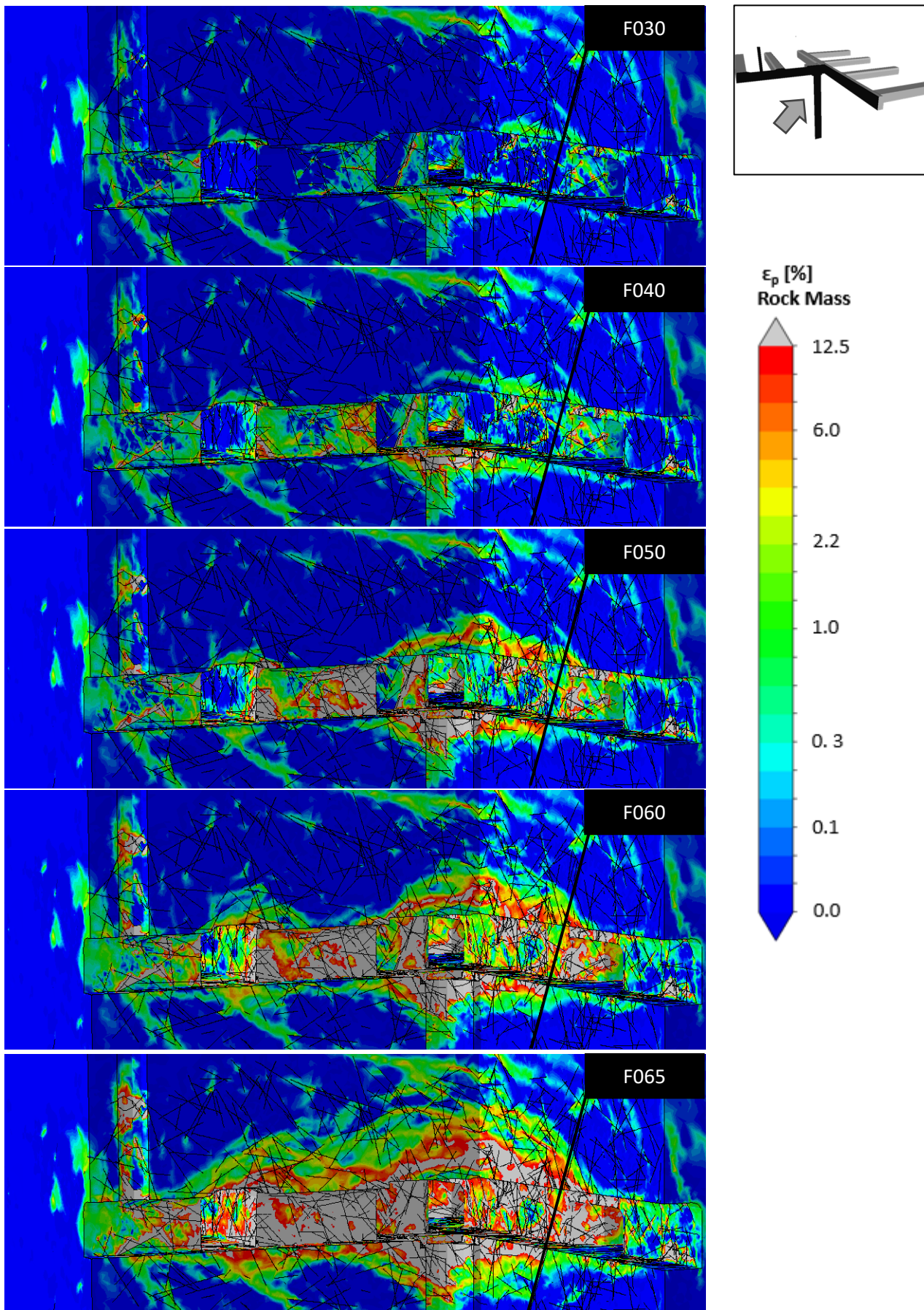
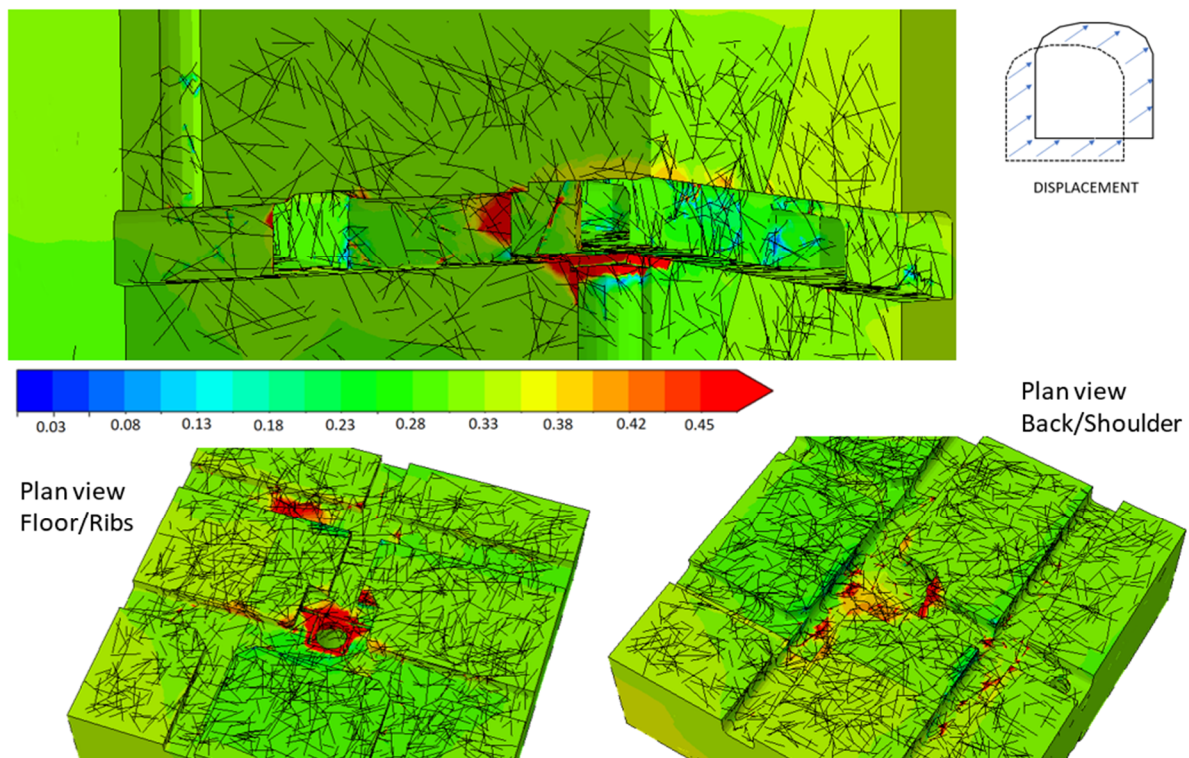


Figure 4 Evolution of mining-induced plastic strain (%) around the excavations, used as a proxy for damage



The simulation also indicates that the whole grizzly precinct and immediate excavations move toward the cave as the cave matures. Figure 5 shows a snapshot of accumulated displacement in F056 as an example. The global translation in this figure is ~250 mm. This magnitude does not necessarily affect the grizzly operation unless relative local displacements or damage associated with global rotations lead to excessive closure and potential failure.

The first sign of potentially impactful relative displacement (>250 mm) occurs at the orepass entry. As caving progresses, displacements then extend to the backs and ribs (Figure 6). Cross marks in Figure 6 show the sampling locations for computing closure. Local relative displacements or closure in this plot are calculated as the distance between two opposite points on either side of the excavation walls. Figure 7 shows the history of closure forecast data with respect to model frame at selected locations. The ribs at the intersection of the grizzly chamber and the crosscut exceed 250 mm closure at F042.



**Figure 5** Global translation of the grizzly precinct due to caving, F056

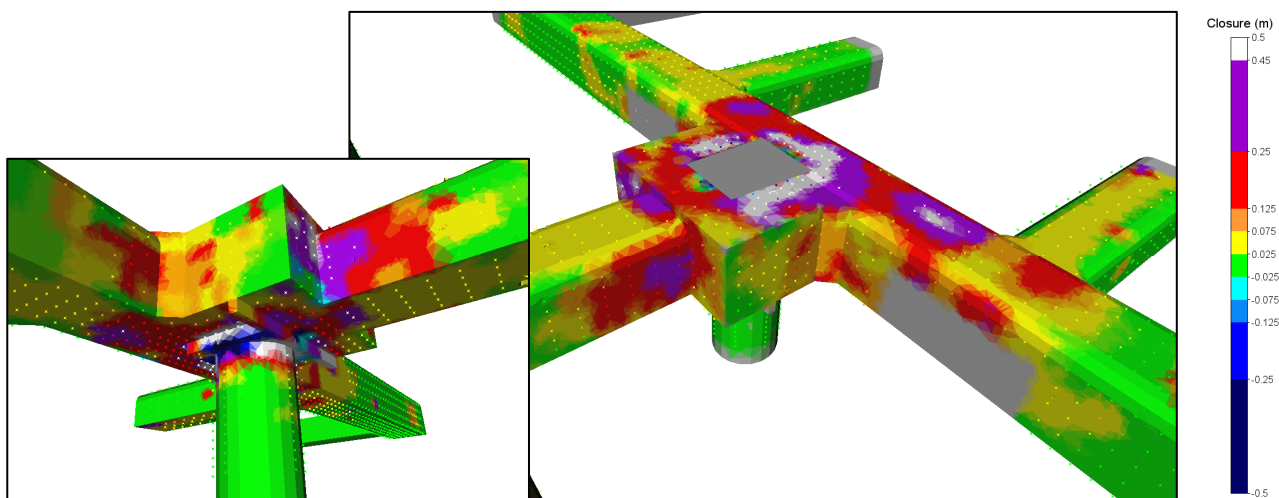


**Figure 6** Relative displacement or closure forecast around the excavations, F056

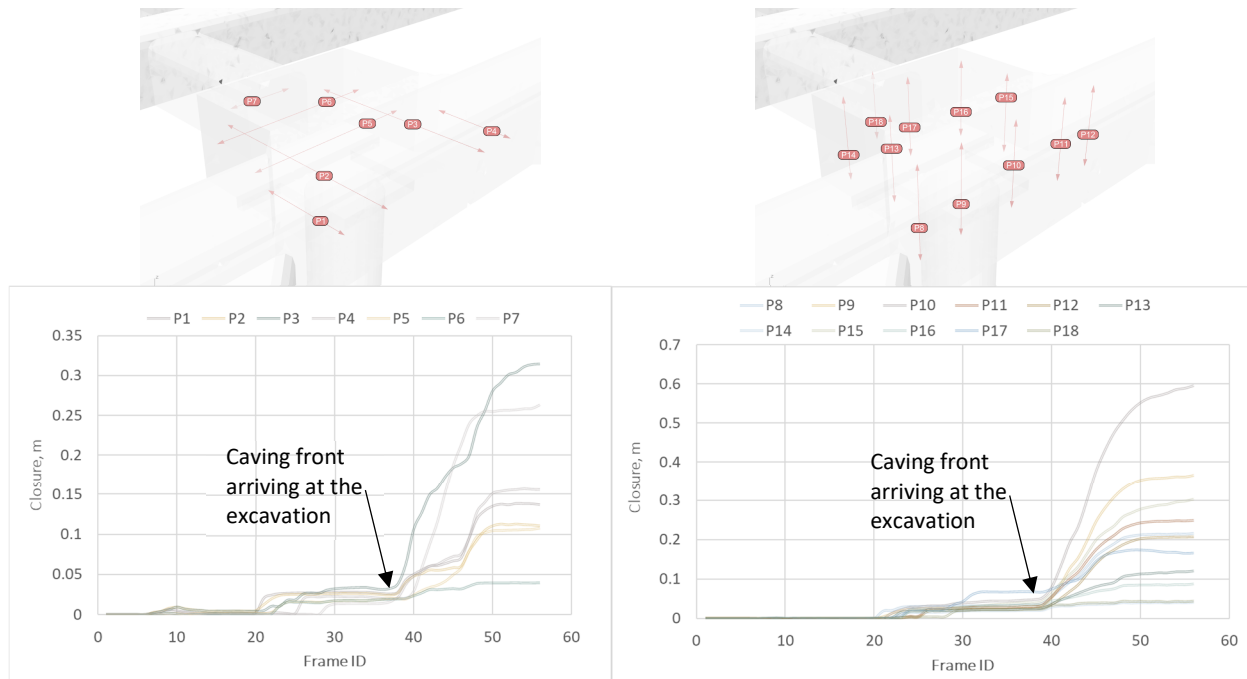


**Figure 7** Closure plots for selected history points in the area of interest

### 3.2 Support performance of rockbolts and cable bolts

Accumulation of axial strain due to ground deformation along the resin bars and cable bolts are shown in Figures 8 and 9, respectively. The high strain spots are initiated by DFNs and grow as depth of damage zone increases. The comparison of depth of rock mass damage and loading points on the cables and bolts can be used to assess the adequacy of the design.

The state of consumed capacity is assessed based on elongation or axial displacement of the bolts. For this purpose, elongation in individual bolts is calculated and tracked in every simulation frame. Elongation thresholds, developed in line with mine’s ground support standard, are used to monitor the capacity consumption. Table 5 shows the evaluation criteria used in this study for cable bolts. Consumed capacity values are calculated based on 6.3% typical elongation at yield for cable bolts and 2,000 m allowance for depth of failure or de-bonded length of the bolts. Figure 10 shows evolution of support capacity consumption in cable bolts in selected simulation steps.

**Table 5** Thresholds and criteria for support consumption in cable bolts

Elongation (mm)	Axial strain (%)	Consumed capacity (%)
25	1.3	20
50	2.5	40
75	3.8	60
95	4.8	75
125	6.3	100
190	9.5	150
250	12.5	200

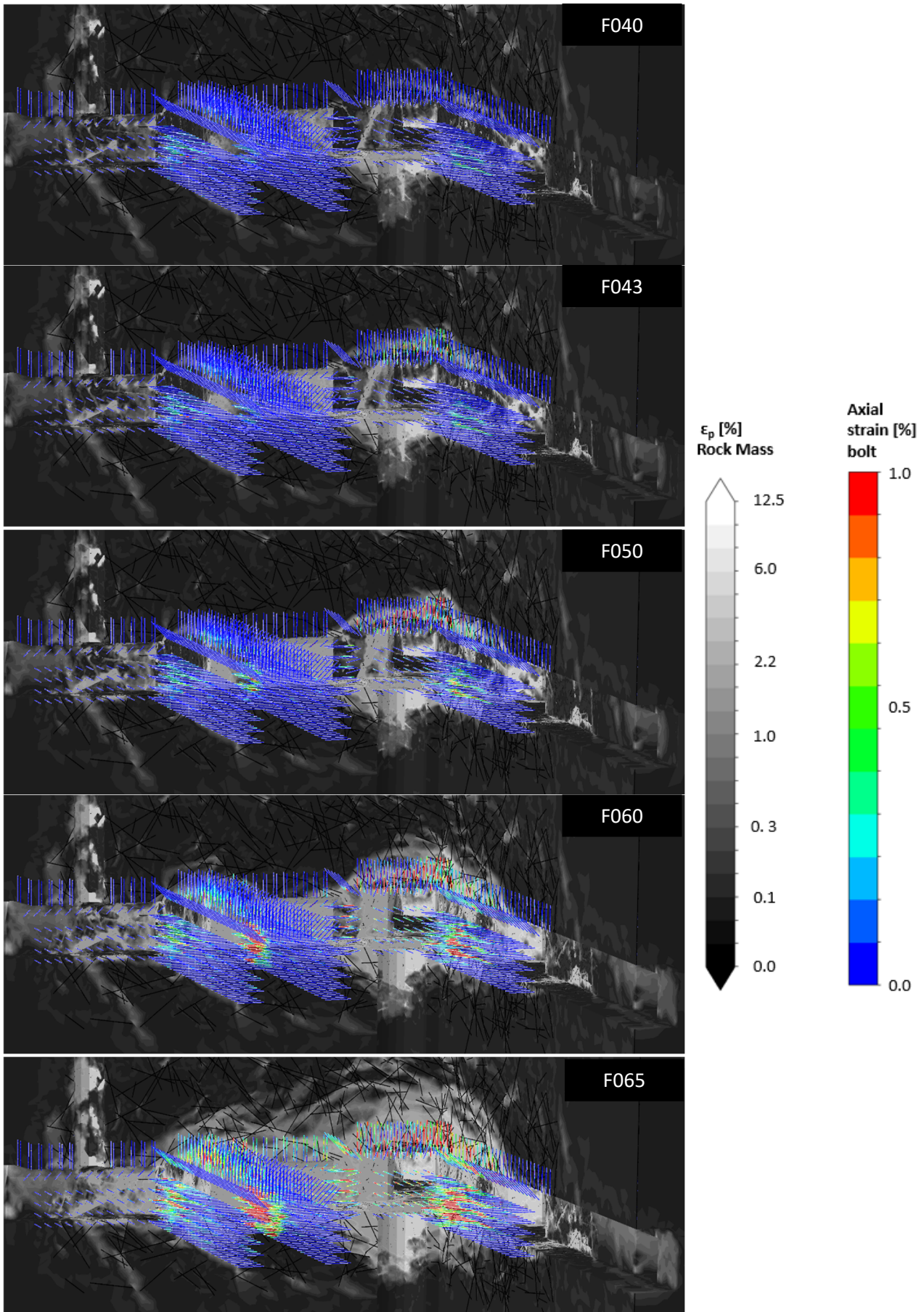


**Figure 8 Simulated strain accumulation in resin bars with progression of induced damage**

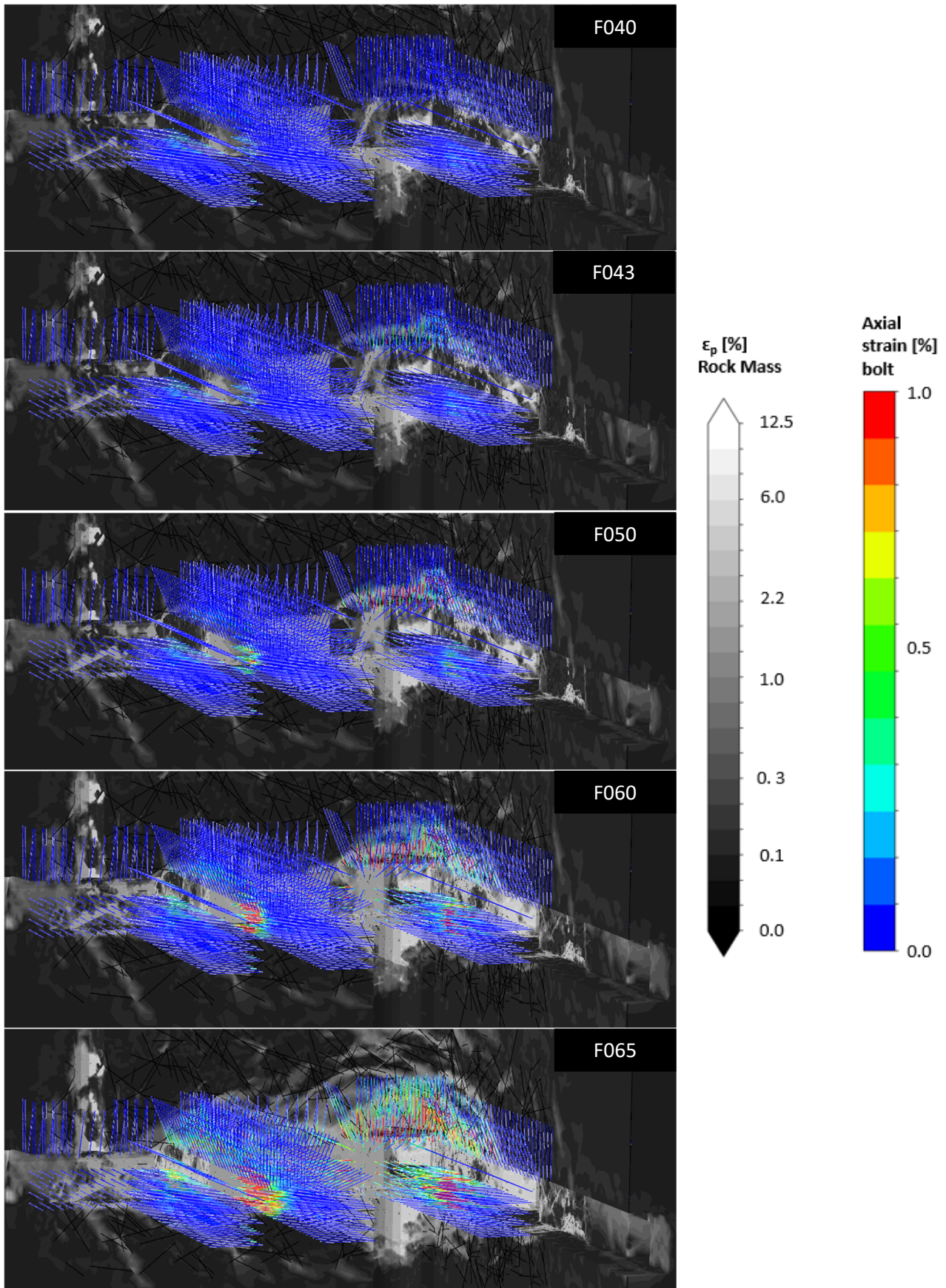
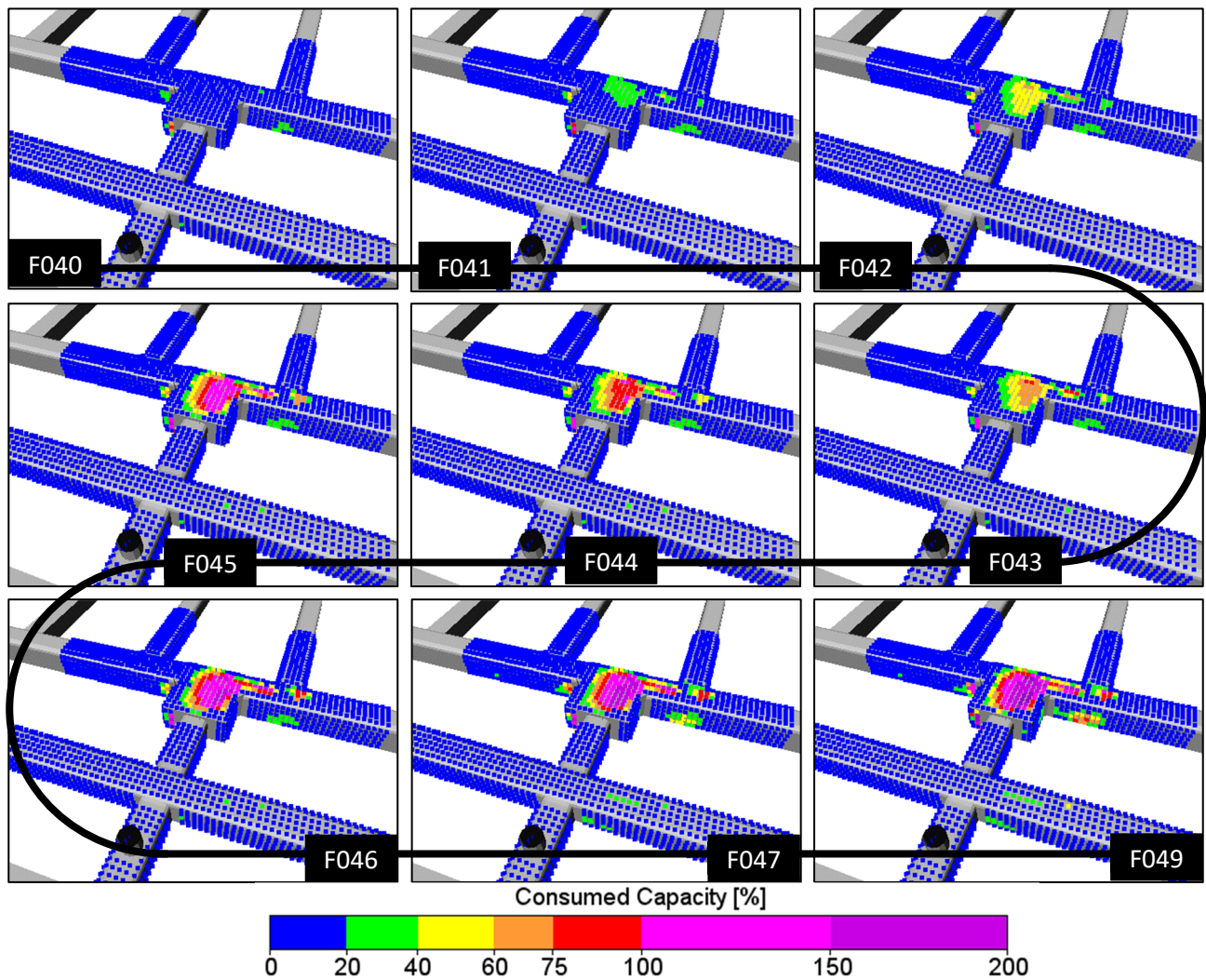


Figure 9 Simulated strain accumulation in cable bolts with progression of induced damage



**Figure 10 Support capacity consumption in selected simulation steps**

For quantitative analysis of support performance, a strain-based criterion was developed (Table 6). The criterion defines three performance levels:

1. **Support:** upon installation, all bolts/cables provide support capacity – the ability to sustain a static load with minimal displacement. A limit of 3.5% total axial strain was adopted for support capacity in both cables and resin bars, as per experience and typical practice. Note 3.5% is typical minimum elongation in cables and bolts before any fracture can take place and the support capacity is diminished, rather than the capacity of the steel element.
2. **Reinforcement:** when multiple adjacent bolts exceed 3.5% strain, they lose capacity but retain reinforcing capacity – load is still required to displace the bolts, which means the bolts continue to mobilise internal friction in the rock mass. The upper limit for reinforcement capacity was selected as 6.3% for cables and 7.5% for resin bars. These values are guided by typical elongation performance before rupture/loss becomes too frequent.
3. **Failure:** once cables or bolts exceed the reinforcement capacity (axial strain of 6.3% for cables and 7.5% for resin bars) the bolts are considered failed. Note this is not the limit at which pervasive drive failure or collapse would be expected. This rating is the limit beyond which the support element is no longer contributing to the system.

**Table 6 Strain-based criterion for evaluating state of rock and cable bolts**

State	Rockbolt	Cable
Support capacity limit	$\epsilon < 3.50\%$	$\epsilon < 3.50\%$
Reinforcement capacity limit	3.5–7.5%	3.5–6.3%
Lost capacity	$\epsilon > 7.5\%$	$\epsilon > 6.3\%$

Figures 11 and 12 show the rockbolts and cable bolts exceeding the support limit and residual reinforcement capacity in every model frame. In summary:

- Isolated resin bars at the ribs of the grizzly chamber lose support capacity in F039 and exceed reinforcement limit in F040.
- Isolated cable bolts at the ribs of the grizzly chamber lose support capacity in F041 and exceed reinforcement limit in F043.
- Some resin bars and cables in the backs surpass support and residual limits in F042 and F043 respectively.
- The closure limit for exceeding support capacity is approximately 125–180 mm and for residual capacity is 180–300 mm.

Further detailed statistical analyses are conducted to determine the clustering of failed rock and cable bolts at every model frame. The clustering has been assessed in four categories:

1. Single isolated bolts.
2. Two adjacent bolts.
3. Three to four adjacent bolts.
4. More than five bolts.

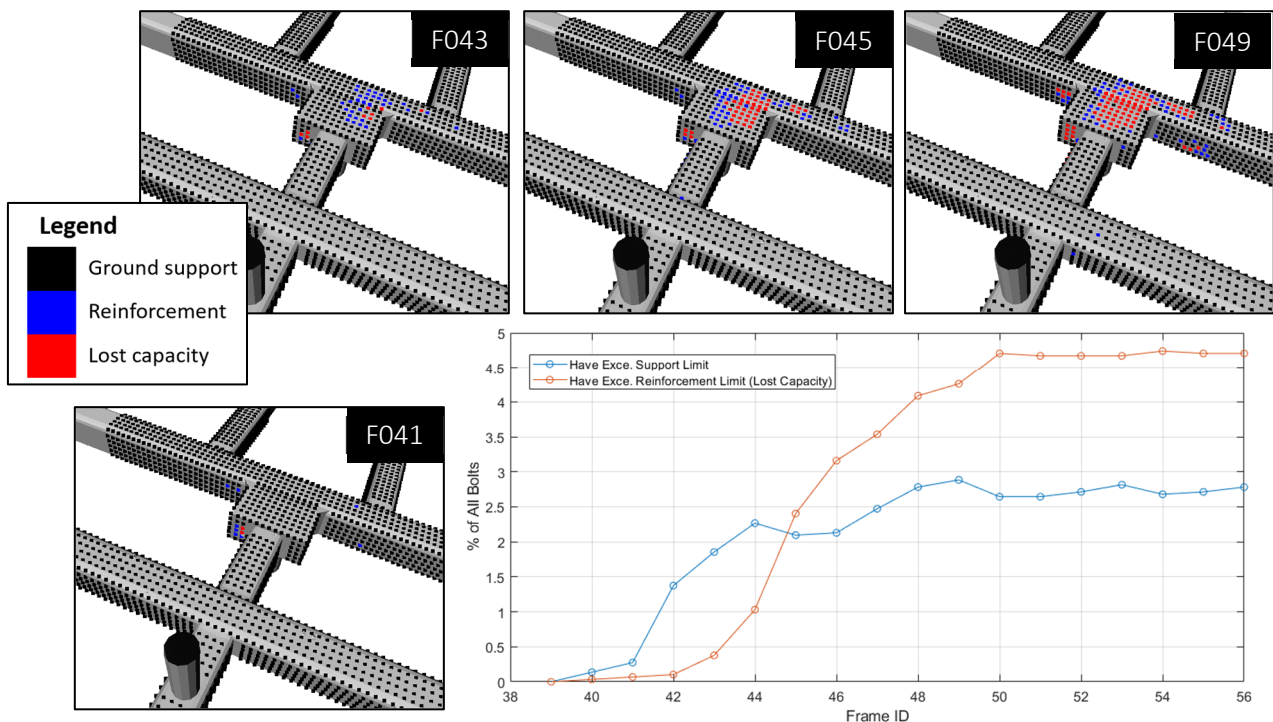


**Figure 11 Quantitative analyses of cable bolt performance – 2,919 resin bars in total**

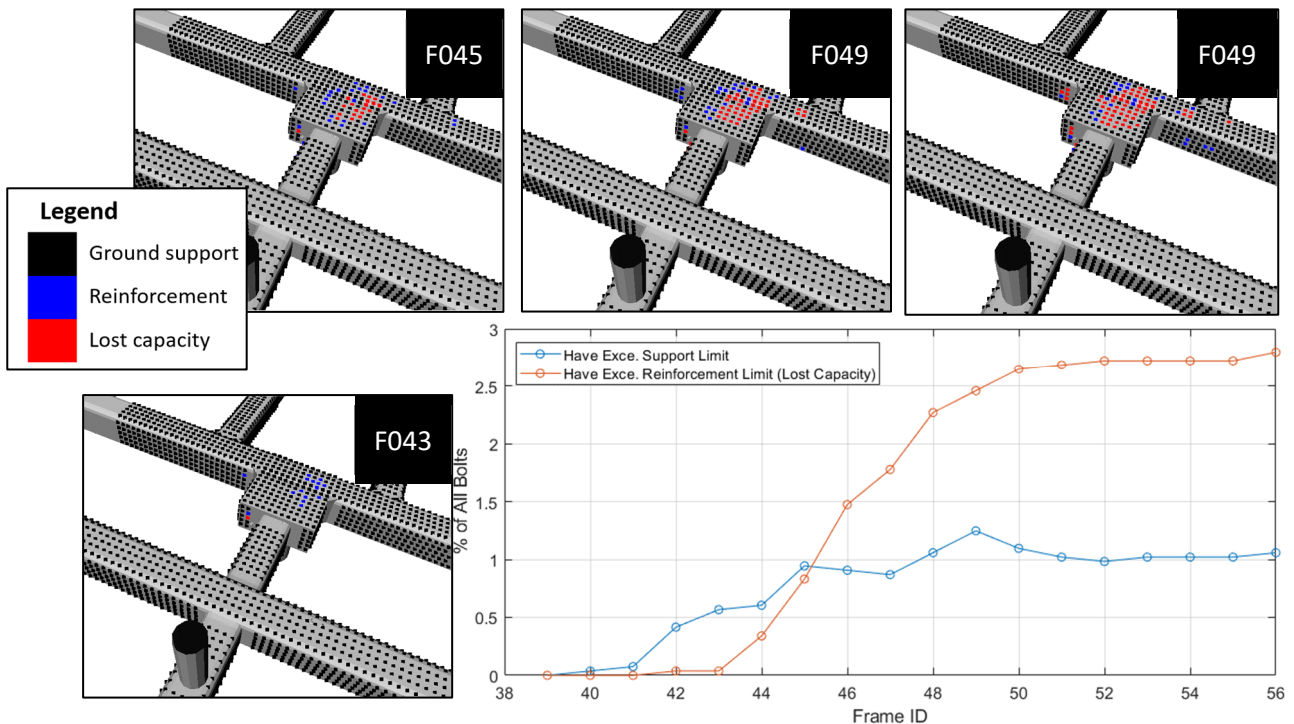


**Figure 12 Quantitative analyses of cable bolt performance – 2,446 cable bolts in total**

Overall, clustering of more than two damaged cable bolts and more than three rockbolts will require action. Figure 13 shows the results for selected frames. These sorts of analyses not only identify the weakness of the ground support design but can also guide the development of a preventative ground support maintenance plan. By providing a quantitative tool to assess performance of the support system over the life of mine, the outcome set guides to when and where preventative measures will be required. The results also allow identification of high-risk areas and define deformation trigger levels based on forecast closure data (Figures 6 and 7) beyond which entry into an excavation with a particular support design would need to be reviewed.

### 3.3 Damage evolution in surface support system

Damage to the surface support (fibrecrete and mesh compound) was assessed based on maximum in-plane principal strain within the excavation shell. Figure 14 shows evolution of damage to the surface support at various stages of caving. The results show fine cracks appear in fibrecrete ribs and corners of the grizzly due to minor displacements along sub-excavation defects (DFN). These cracks continue extending and widening as caving progresses, leading to potential slabbing. Overall, the modelling shows that the surface support is moderately damaged at between 25–75 mm of closure and very significantly damaged between 75–135 mm of wall-to-wall closure.

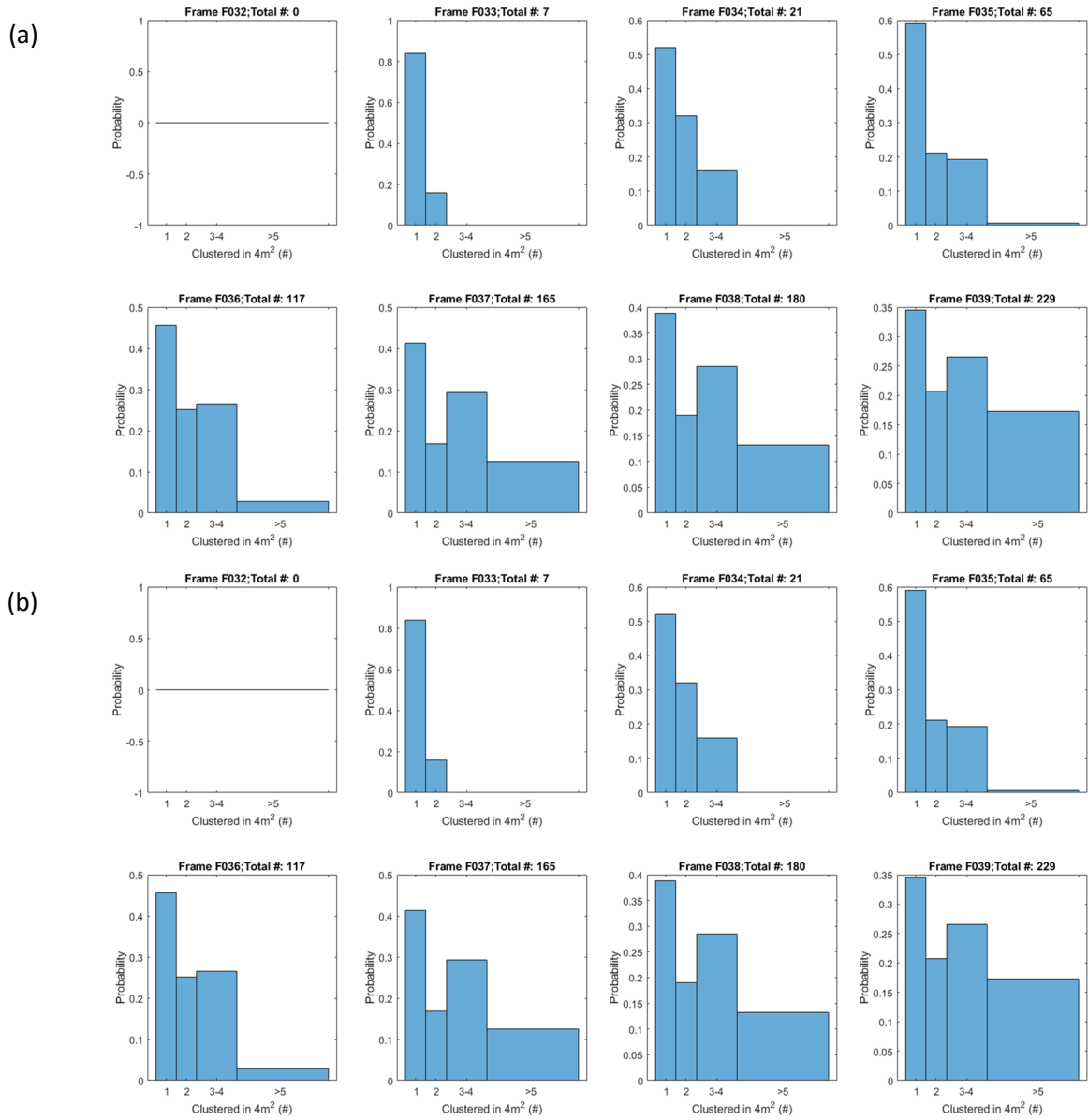


Figure 13 Statistics of clustering of failed. (a) Rockbolts; (b) Cable bolts at each simulation frame

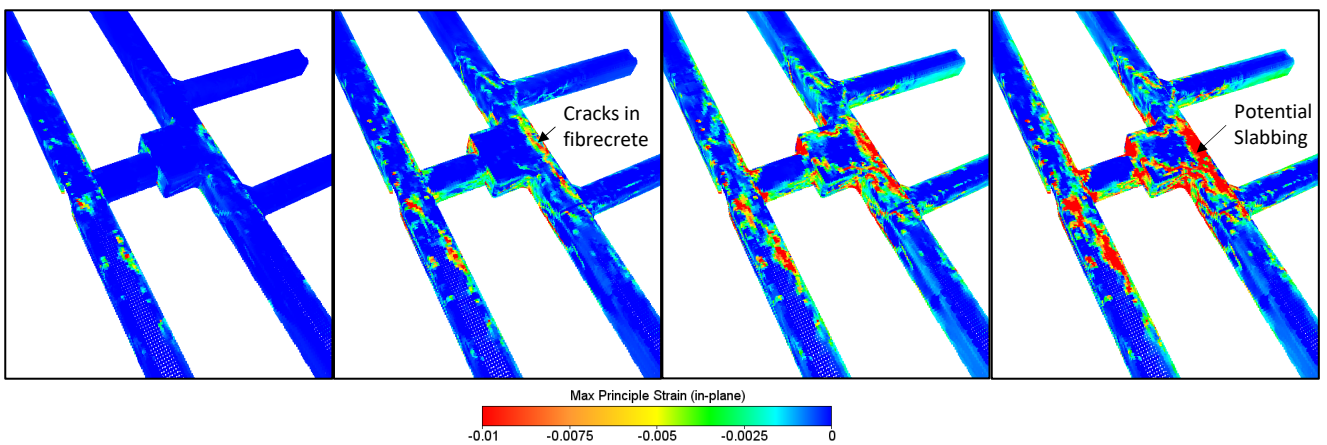


Figure 14 Strain accumulation in surface support with induced damage



## 4 Conclusion

A numerical modelling technique was used to forecast and assess performance of ground support systems over the life of underground mining excavations. The scope required high similitude with displacements and the distribution of damage around excavations with a resolution to a sub-bolt length scale, so considerable care was taken in the construction and formulation of the rock mass defects, excavation sequencing and constitutive formulation of the sub-models.

The support system was simulated in a discontinuous rock mass subjected to a mining-induced stress and strain path. The developed methodology tracked the consumed and the remaining capacity of the individual support elements within the system as loading demand increased and deformation occurred. By providing a quantitative tool to assess performance of the support system over life of mine, the outcome assists the mines to set guides to when and where preventative measures will be required. The results combined with closure forecast data also allow identifying high-risk areas and deformation trigger levels beyond which entry into an excavation with a particular support design would need to be reviewed. A qualified and competent engineer can use these outcomes to adjust the timing of the preventative maintenance as needed to account for exposure and other operational needs following regulatory requirements, company standards and assurance frameworks. To ensure that maintenance occur as needed, a monitoring program overseen by a qualified engineer is needed.

## References

- Hoek, E & Brown, ET 2019, 'The Hoek–Brown failure criterion and GSI – 2018 edition', *Journal of Rock Mechanics and Geotechnical Engineering*, vol. 11, no. 3, pp. 445–463.
- Kaiser, PK & Moss, A 2022, 'Deformation-based support design for highly stressed ground with a focus on rock burst damage mitigation', *Journal of Rock Mechanics and Geotechnical Engineering*, vol.14, no. 1, pp. 50–66.
- Levkovitch, V, Reusch, F & Beck, D 2010, 'Application of a non-linear confinement sensitive constitutive model to mine scale simulations subject to varying levels of confining stress', in J Zhao, V Laboure, J-P Dudt & J-F Mather (eds), *Rock Mechanics in Civil and Environmental Engineering*, CRC Press, Boca Raton.
- Lowther, R, De Ross, J, Orrego, C & Cuello, D 2022, 'A probabilistic evaluation of the displacement-based ground support design approach', in Y Potvin (ed.), *Caving 2022: Fifth International Conference on Block and Sublevel Caving*, Australian Centre for Geomechanics, Perth, pp. 241–254, [https://doi.org/10.36487/ACG\\_repo/2205\\_15](https://doi.org/10.36487/ACG_repo/2205_15)
- Munjiza, A 2004, *The Combined Finite-Discrete Element Method*, John Wiley & Sons, Hoboken.

